Velocity space diffusion of ions in controlled turbulence

Ryohei Itatani, Yasuyoshi Yasaka, and Osamu Fukumasa

Department of Electronics, Kyoto University, Kyoto, Japan
(Received 18 December 1975; final manuscript received 5 August 1976)

The velocity space diffusion of ions due to ion wave turbulence is investigated experimentally using an ion wave echo. Experiments are so arranged that the streaming perturbation due to the first excited wave propagates through the localized region where the ion wave turbulence is excited, to interact with the second excited wave. The resultant second order ion wave echo damps in comparison with the case of no turbulence. The variation of the echo amplitude as the power of the spectrum of the turbulence is changed is observed, which is in quantitative agreement with the theoretical prediction. It is also revealed that the turbulent waves are far more effective than the monochromatic waves in increasing the effective collisions.

I. INTRODUCTION

The velocity space diffusion of ions due to effective collisions is important not only in fundamental physics but in the search for efficient plasma heating. It is expected that effective collisions will be very useful in preventing the decrease in the power absorption rate of a plasma even at high temperatures. In practice, turbulent heating experiments[1] have often achieved anomalous heating, which indicates that the effective collisions of particles with turbulent waves play an important role in the thermalization process.

Here, we are concerned with the velocity space diffusion of ions in externally controlled ion wave turbulence. The measurement technique we employ is to use an ion wave echo as a probe wave. Plasma wave echoes have been predicted to be useful in investigating the effects of diffusion due to collisions or turbulence.[2,3] From this point of view, several experimenters studied the effects of Coulomb collisions on electron[4,5] or ion wave echoes.[6-8] Moeller[5] has obtained the velocity dependence of diffusion coefficients using the Fourier transform of measured echo amplitudes. In experiments performed by Jensen *et al.*[9] and Guillemot *et al.*,[10] electron wave turbulence was introduced into the plasma and the variation of the electron wave echo due to the change in applied noise power was measured. Their results have shown good agreement with quasilinear theory. Nevertheless, an experimental report dealing with the effects of ion wave turbulence on ion wave echoes is not yet available.

Our experiments were performed in such a way that the streaming perturbation due to the first excited wave propagates through the localized region where the ion wave turbulence is excited, to interact with the second excited wave. The resultant second order ion wave echo amplitude reduces in comparison with the case of no turbulence. We observed the variation of the echo amplitude as the power or the spectrum of the turbulence was changed. The experimental results are in quantitative agreement with the theoretical prediction on the basis of the generalized quasilinear theory.

The theory is described in Sec. II. Sections III and IV contain the experimental methods and results, respectively. Section V deals with the discussion including the comparison between experiments and the theory. The conclusions are presented in Sec. VI.

II. THEORY

As is well known, the plasma wave echo appears as a result of the interaction between the streaming perturbation due to the first excited wave and the electric field of the second one. Here, we show the effect of ion wave turbulence on the second order ion wave echo by means of generalized quasilinear theory in a one-dimensional and uniform plasma.

The streaming perturbation of the ion velocity distribution function resulting from the ion wave of the frequency ω_1 excited at $x=0$ is written as

$$f_{\omega_1}(x, v) = -i\frac{e}{M}\frac{\Phi_1}{\epsilon(\omega_1/v, \omega_1)}\frac{1}{v}\frac{\partial f_0}{\partial v}\exp\left(i\frac{\omega_1}{v}x\right), \tag{1}$$

where Φ_1 is the first applied potential and $\epsilon(k, \omega)$ is the dielectric function with k $(\equiv k_R + ik_I)$ being the wavenumber. Coulomb collisions affect this streaming perturbation and damp it. The correction of f_{ω_1} due to the collisions will be done later [see Eq. (6)].

If the ion wave turbulence generated at $x=l_1$ by the externally applied noise has the spatial dependence of the form

$$\Phi(x, t) = \int d\omega' \psi_{\omega'} \exp[ik(\omega')(x-l_1) - i\omega' t], \tag{2}$$

the Vlasov equation which determines the behavior of f_{ω_1} takes the form,[3]

$$-i\omega_1 f_{\omega_1}(x, v) + v\frac{\partial}{\partial x} f_{\omega_1}(x, v) - \left(\frac{e}{M}\right)^2 \int d\omega' \frac{\partial \Phi_{\omega'}(x)}{\partial x}$$
$$\times \frac{\partial}{\partial v}\left\{\int_{l_1}^{x} d\xi \exp\left[i\frac{\omega_1 - \omega'}{v}(x-\xi)\right]\frac{\partial \Phi_{-\omega'}(\xi)}{\partial \xi}\right.$$
$$\left.\times \frac{1}{v}\frac{\partial}{\partial v} f_{\omega_1}(\xi, v)\right\} = 0, \quad (x \geq l_1) \tag{3}$$

where $\Phi_\omega(x)$ is the Fourier transform of $\Phi(x, t)$. Assuming that the main contribution of the velocity derivative comes from the part acting on the exponential term of f_{ω_1}, we solve Eq. (3) to find

$$f_{\omega_1}(x, v) = \bar{f}_{\omega_1}(v)\exp\left[i\frac{\omega_1}{v}x - \frac{1}{v}\int_{l_1}^{x} dx' G(x', v)\right], \tag{4}$$

where

$$G(x', v) = \frac{\omega_1^2 x'}{v^5}\left(\frac{e}{M}\right)^2 \int d\omega' \left| k(\omega')\right|^2 \left|\Phi_{\omega'}(x')\right|^2$$

$$\times \int_{l_1}^{x'} d\xi\, \xi \exp\left\{-i\left[k(-\omega') + \frac{\omega'}{v}\right](x' - \xi)\right\}, \tag{5}$$

and $\bar{f}_{\omega_1}(v)$, which is the slowly varying function of v, can be determined by the boundary condition that Eq. (4) reduce to Eq. (1) at $x = l_1$.

The electric field associated with the second wave of the frequency ω_2 launched at $x = l$ interacts with the perturbation expressed in Eq. (4), to produce the second order ion wave echo at the frequency $\omega_3 = \omega_2 - \omega_1$. The second order perturbation in the neighborhood of the echo peak is, including Coulomb-collisional damping,[3]

$$f_{\omega_3}(x, v) = \bar{f}_{\omega_3}(v) \exp\left[i\frac{\omega_3}{v}(x - l^*) - \frac{\omega_1^2 \omega_2 l^3}{3\omega_3 v^5} D_2(v)\right.$$

$$\left. - \frac{1}{v}\int_{l_1}^{l} dx'\, G(x', v)\right], \tag{6}$$

where $l^* = (\omega_2/\omega_3)l$ is the location of the echo, and $D_2(v)$ is the coefficient of velocity space diffusion due to Coulomb collisions. The third term in the exponent represents the damping effect of the ion wave turbulence which is externally excited at $x = l_1$. In deriving Eq. (6), it is assumed that the turbulence damps away beyond $x = l$. Substituting Eq. (6) into Poisson's equation, we obtain the peak echo potential

$$\Phi_{\omega_3}(x = l^*) = \frac{e}{M}\frac{\omega_2^2 \Phi_1 \Phi_2 \omega_1 l}{\pi^{1/2} v_t^3 \omega_3^2}\int \frac{dv}{v}$$

$$\times \frac{\exp -\left[\left(\frac{v}{v_t}\right)^2 + \left(\frac{\omega_1^2 \omega_2 l^3}{3\omega_3 v^5}\right) D_2(v) + \left(\frac{1}{v}\right)\int_{l_1}^{l} dx'\, G(x', v)\right]}{\epsilon(-\omega_1/v, -\omega_1)\epsilon(\omega_2/v, \omega_2)\epsilon(\omega_3/v, \omega_3)}, \tag{7}$$

where ω_p is the ion plasma frequency, v_t is the ion thermal velocity, and f_0 contained in Eq. (6) through $\bar{f}_{\omega_3}(v)$ is replaced by the Maxwellian.

The saddle point integration of Eq. (7) is adequate for the evaluation of Φ_{ω_3}, since the pole contribution to the integral is very weak for heavily damped waves such as in our case. The first two exponential terms in the integrand become a maximum at the velocity v_s which is given by Eq. (11) of Ref. 7 after the appropriate substitution for $D_2(v)$. Even when the third exponential term exists, the integrand is peaked at v_s for the reason that the third term in the exponent is smaller by an order of magnitude than the others and that the phase velocity v_p ($\equiv \omega/k_R$), at which the third term is peaked as seen in Eq. (5), coincides with v_s for our experimental condition. Thus, we can perform the saddle point integration of Eq. (7) using v_s, and find that the maximum amplitude of the echo is reduced due to the ion wave turbulence by the factor

$$\exp(-K_i) \equiv \exp\left[-\frac{1}{v_s}\int_{l_1}^{l} dx'\, G(x', v_s)\right], \tag{8}$$

where $v_s \simeq v_p$.

The following substitution is convenient for the calculation of Eq. (8)

$$\left|\Phi_\omega(x)\right|^2 = \eta^2 \langle V_x^2\rangle\, S(\omega, \omega_0) \exp[-2k_I(x - l_1)]. \tag{9}$$

Here, $\langle V_x^2\rangle$ is the time averaged square of the externally applied noise voltage, η is the coupling coefficient of the grid, and $S(\omega, \omega_0)$ is the power spectrum of the turbulence at $x = l_1$. In Sec. V, we shall calculate Eq. (8) using Eq. (9) in order to compare with the experimentally observed damping factor K_i.

III. EXPERIMENTAL METHODS

The experiments were performed in a single-ended Q machine of a potassium plasma. The schematic diagram of the experimental arrangement is shown in Fig. 1. The plasma was produced by surface ionization of a beam of potassium atoms on a hot tungsten plate heated to about 2200 °K by electron bombardment. The plasma formed a column 3 cm in diameter and 1.3 m long in an axial magnetic field of intensity up to 10 kG. The plasma density and the electron temperature as measured by the Langmuir probe, were $n_0 = (0.2 \sim 1) \times 10^9$ cm^{-3} and $T_e \simeq 0.25$ eV, respectively. The ion temperature, which was roughly estimated from the propagation and damping of ion waves,[11] was close to T_e. The background neutral gas pressure was lower than 2×10^{-6} Torr. At this pressure the mean free paths for ion-neutral and electron-neutral collisions are much longer than the length of the plasma column.

Four grids made of 0.05 mm diam tungsten wires spaced about 3 mm apart, were immersed in the plasma with their surfaces perpendicular to the axis. Two of them, G_1 and G_2 with separation l, were used as exciters of ion acoustic waves of frequencies f_1 and f_2, respectively. The echo was received on the grid G_D which was movable in an axial direction. Signals from G_D were fed to a phase sensitive detector together with the reference signal $f_2 - f_1$. The fourth grid G_N which was set at a distance 2 cm upstream from G_2, generated turbulent fields in the plasma. This grid was connected through a low pass filter to a wide band noise generator. The power spectrum of the turbulence can be controlled by varying the cutoff frequency of the low pass filter.

Signals from each grid were also analyzed by a correlator. Namely, the fluctuating part of a voltage across a detection resistor through which the ion saturation current detected on one of the grids flows, was fed to the correlator. The input voltage to the correlator is proportional to the fluctuating potential in the plasma. The proportional constant can be obtained provided the

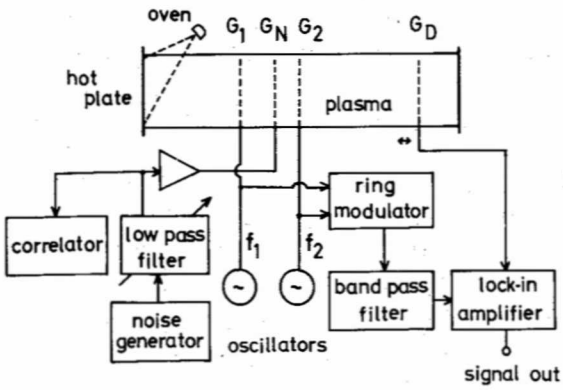

FIG. 1. Schematic of the experimental arrangement.

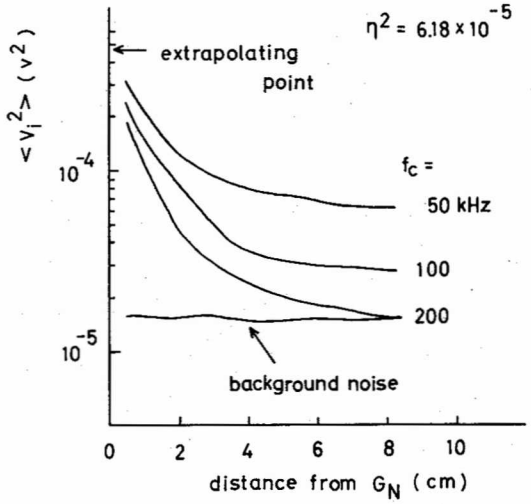

FIG. 2. Spatial evolution of the power of the excited turbulence. Noise signals with the power of 7.5 V^2 are applied through the low pass filter with the cutoff at 50, 100, and 200 kHz.

electron temperature and the dc part of the ion saturation current are monitored with the proper choice of the detection resistor. The proportional constant was 1.67 when the electron density was kept at 0.56×10^9 cm^{-3} with a resistance of 1 kΩ. Thus, we can measure the absolute value of the fluctuating potential in the plasma.

IV. EXPERIMENTAL RESULTS

A. Spatial evolution of excited turbulence

In the first part of the experiment, the characteristics of the excited ion wave turbulence are examined. Measurements were made in such a way that the fluctuating potential detected on the grid G_D was fed to the correlator using the method described in a previous section, to compute auto-correlation functions. The turbulence was excited from G_N, and the grid G_2 was removed in this case.

Figure 2 shows the spatial evolution of the time averaged power of the turbulence generated by the noise whose power spectrum is varied through the low pass filter with the cutoff frequency f_c. The abscissa is the distance from G_N, and the mean squared voltage of the applied noise is kept at $\langle V_x^2\rangle = 7.5\ V^2$ in all cases of f_c.

It is apparent from Fig. 2 that the turbulence having higher frequency components decays more rapidly in space. As shown in Sec. II, a coupling coefficient η which relates the mean squared potential in the plasma to that of the externally applied noise signals is defined as

$$\langle V_i^2(x=l_1)\rangle = \eta^2\langle V_x^2\rangle, \tag{10}$$

where the angular brackets ($\langle\ \rangle$) denote time average. (At $x=l_1$, the level of the background noise is negligible as compared with that of the excited turbulence.) We estimated the value of $\langle V_i^2(x=l_1)\rangle$ to be $4.64\times10^{-4}\ V^2$ by extrapolating the curves in Fig. 2 to the point of $x=l_1$ (i.e., origin of the abscissa). Then, the value of η^2 can be obtained through Eq. (10), which was found to be 6.18×10^{-5} regardless of the cutoff frequency used so far. Of course, η is dependent on the plasma density and the spacing of the grid meshes. The measured value was obtained at a density of $n_0 = 0.56\times10^9$ cm^{-3}.

In Fig. 2, the lowest curve exhibits the case of no noise applied. It can be seen that the plasma has the spatially homogeneous background noise with the frequency range up to several kHz.

In order to obtain the phase velocity of the turbulence a cross-correlation function of excited noise signals detected on G_N and G_D was computed. The time for the cross-correlation to become a maximum is plotted against the separation between two grids in Fig. 3. The linear dependence of the time for maximum correlation on the grid separation shows that the phase velocity of the turbulence is 2.23×10^5 cm/sec. It corresponds to the measured phase velocity of ion acoustic waves. Hence, we see that the excited turbulence is of the ion acoustic mode. The same procedure was applied to the background noises, to reveal that one of the modes is the ion acoustic mode. A drift-wave-like noise was also observed.

B. Test wave propagation

A small amplitude test wave of ion acoustic mode was launched from G_2 in the ion wave turbulence excited from G_N. The spatial damping decrement of the test wave k_I is plotted against the wave frequency f in Fig. 4.[12] In the absence of externally applied noise, the damping decrement is proportional to f^α with $\alpha = 0.982\pm0.01$, and the damping rate k_I/k_R is 0.22 regardless of the frequency. We obtained the constant α by applying the method of least squares to several tens of wave-pattern data. These results confirm the linear theory of collisionless damping. If the ion wave turbulence is excited with the noise signals of $\langle V_x^2\rangle = 7.5\ V^2$ and $f_c = 200$ kHz, the phase velocity of the test

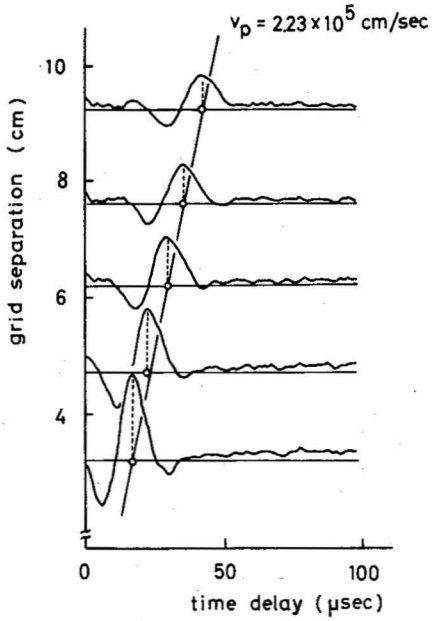

FIG. 3. Cross-correlation functions for several grid separations. The plot of the time for maximum correlation versus the separation reveals the phase velocity of the turbulence to be 2.23×10^5 cm/sec.

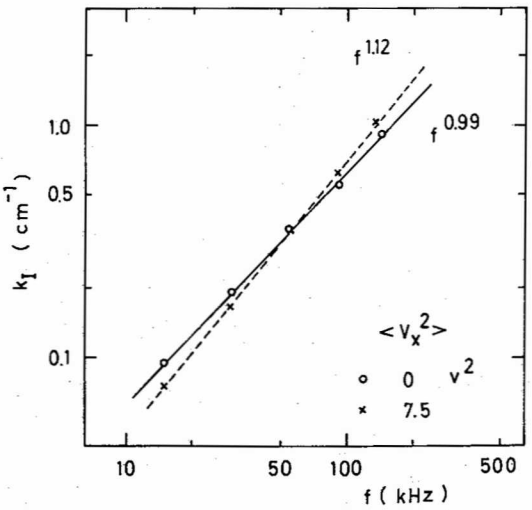

FIG. 4. The spatial damping decrement of the test wave with (dotted line) and without the excited turbulence (solid line) versus the wave frequency.

wave remains constant, but the damping decrement now follows the relation,

$$k_I = k_0 (f/f^*)^{1+\beta}, \tag{11}$$

where $k_0 = 0.36\ \mathrm{cm}^{-1}$, $f^* = 60$ kHz, and $\beta = 0.13 \pm 0.02$. This relation approximately holds in the range where $6.5 < \langle V_x^2 \rangle < 13.0\ \mathrm{V}^2$ and $f_c > 50$ kHz. When the power of the turbulence was decreased less than $6.5\ \mathrm{V}^2$ or f_c was chosen below 50 kHz, the damping decrement tended to follow the linear relation with f. The deviation of the damping from the linear Landau damping may be due to the resonant wave-wave interaction.

C. Damping of the echo amplitude

In this section a second order ion wave echo is excited and its amplitude damping due to the turbulence is studied. The measured dispersion relation of echoes corresponds to that of ion acoustic waves, and the echo amplitude is proportional to both the exciting voltages of G_1 and G_2. In what follows we choose the exciting frequencies and voltages such that $f_1 = 80$ kHz, $f_2 = 180$ kHz, $V_1 = 2\ V_{pp}$, and $V_2 = 3\ V_{pp}$.

We measured the peak amplitude of the echo with and without the excited turbulence for a few values of the exciter separation l. The normalized amplitude $A/n_0 l$ is plotted as a function of $n_0^{1/3} l$, as shown in Fig. 5. The mean squared voltage of applied noise was $3.5\ \mathrm{V}^2$ and no filter was used. A variation of the plasma density n_0 was always checked by observing dc ion saturation current to G_D. The exponential decay of $A/n_0 l$ without turbulence versus the exciter separation shows the effect of Coulomb collisions and the background noise.

The effect of the excited turbulence is evidenced by the fact that the echo amplitude is diminished compared with the case of no turbulence, and that with an increase of l, the damping due to the turbulence becomes stronger.

As described in Sec. II, the theory predicts that the damping factor K_i is a function of the power, the spectrum, and the location of the turbulence. We proceed to examine the dependence of the damping of the echo amplitude due to the turbulence on such parameters. The factor K_i was obtained from the measured ratio of the echo peak amplitude with the excited turbulence to that without it, using the relation $K_i = -\ln (A/A_0)$.

Figure 6 gives the value of K_i as a function of the power of the applied noise up to 100 kHz. The value of K_i increases linearly with the power of the applied noise. This result is consistent with the theoretical prediction expressed in Eq. (8). The dependence of the damping factor K_i divided by the external noise power $\langle V_x^2 \rangle$ on the location of G_N is shown in Fig. 7 together with the calculated value. This normalization of K_i is based on the fact that the value of K_i is proportional to the external noise power as shown in Fig. 6. Since the change of l_1 is made by moving the position of G_1, the distance between G_N and G_2 (i.e., the turbulent region) remains unchanged. Figure 7 shows the behavior that the damping factor increases gradually when l_1 is increased with a fixed external noise power. But the l_1 dependence is weaker than those predicted (see Sec. V).

Varying the cutoff frequency of the low pass filter, we further measured the dependence of the damping of

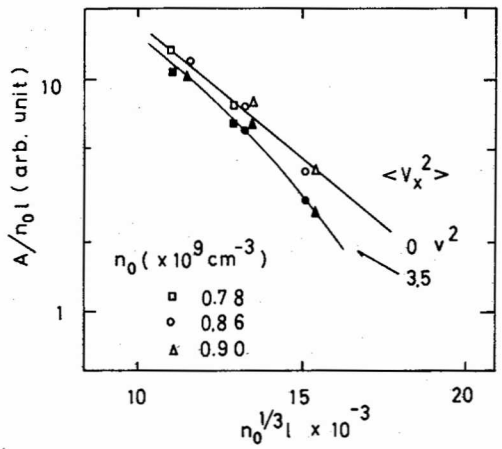

FIG. 5. The peak echo amplitude A divided by $n_0 l$ with and without the excited turbulence versus the normalized distance between G_1 and G_2.

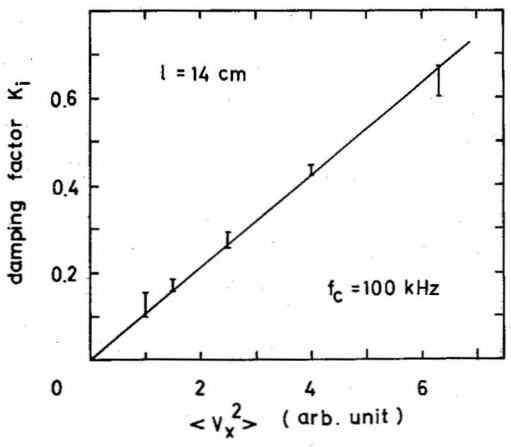

FIG. 6. The damping factor K_i versus the applied noise power. Noise signals are filtered by the low pass filter with the cutoff at 100 kHz.

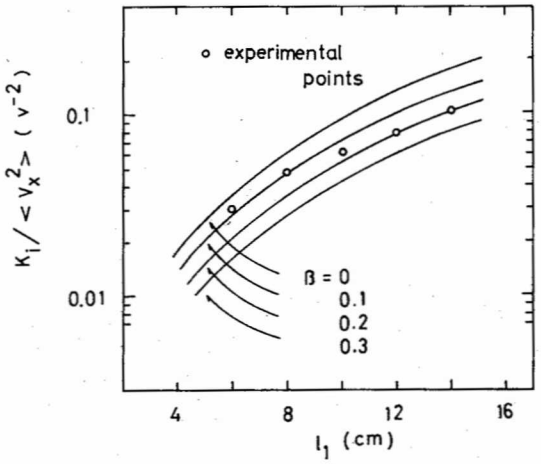

FIG. 7. The damping factor K_i divided by the applied noise power $\langle V_x^2\rangle$ versus the distance between G_1 and G_N. The calculated values are also shown for $\beta=0$, 0.1, 0.2, and 0.3. Other parameters in the calculation are as follows; $k_0=0.36$ cm^{-1}, $f^*=60$ kHz, and $\eta^2=3.4\times10^{-5}$.

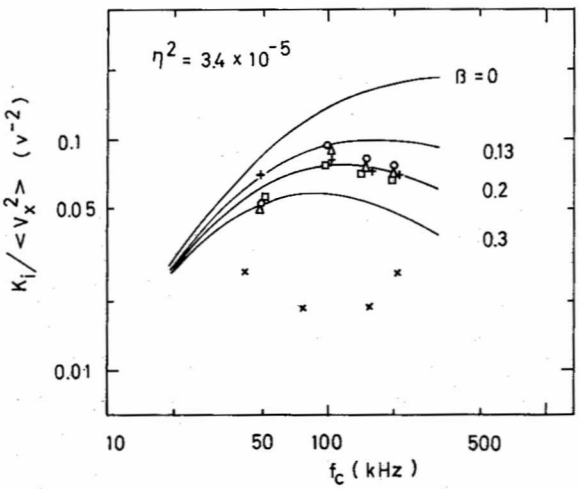

FIG. 9. The damping factor K_i divided by the noise power versus the cutoff frequency of the applied noise (+, ○, △, □) or the frequency of the applied monochromatic signals (×). Solid curves are calculated values for the noise application.

the echo on the spectrum of the turbulence. The results are shown in Fig. 8. The power of the excited turbulence must be unchanged in varying f_c. The parameter z means the distance from G_N at which the internal noise power is kept constant by controlling the external noise power for four values of f_c. The value of A/A_0 exhibits a rather complicated behavior, but plotting $K_i/\langle V_x^2\rangle$ versus f_c yields the display given in Fig. 9. The damping of the echo amplitude for unit power of applied noise is a maximum when the cutoff frequency is at 100 kHz or so.

Then, we applied monochromatic signals with the frequency of f_c to G_N instead of the noise. As denoted by the sign × in Fig. 9, the echo amplitudes are less damped than the case of the noise application by almost a factor of 4.

V. NUMERICAL RESULTS AND DISCUSSIONS

In Fig. 5, we have shown that the logarithm of the normalized echo amplitude decreases proportionally to $n_0^{1/3}l$ when no turbulence is excited. Several different results concerning the l dependence of the ion wave echo amplitudes were reported.[6-8] Theoretical explanations of these were made by using a Fokker–Planck operator as a collision term, but there seems to be no fixed theory which can explain all the results. We think this failure may due to the fact that the effect of the background noise was not taken into account. The existence of the background noise will bring the velocity space diffusion of ions whose velocity is near the phase velocity of the noise. In practice, we observed the decrease of the echo amplitude as the level of the background noise increased. In this case, the l dependence of the echo amplitude deviates from the $l^{3/5}$ behavior[7] which is the case with neither the background nor the external noise. [The saddle point integration of Eq. (7) without the third term in the exponent predicts that the normalized echo amplitude decays exponentially with $l^{3/5}$.] The l dependence with the background noise should be stronger than $l^{3/5}$ because the damping effect of the background noise increases with l.

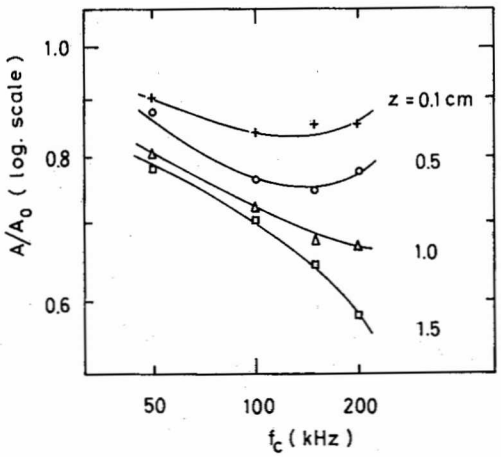

FIG. 8. The ratio of the echo amplitude with the excited turbulence to that without it versus the cutoff frequency of the applied noise. The power of the turbulence at the position z cm downstream from G_N is kept constant to be 2.1×10^{-4} V^2 in varying the cutoff frequency.

We wish to calculate the value of $K_i/\langle V_x^2\rangle$ using Eqs. (8), (5), and (9), which we rewrite as

$$K_i/\langle V_x^2\rangle = \eta^2 F(S, k_I, l, l_1). \tag{8'}$$

The value of F is determined if the power spectrum $S(\omega, \omega_0)$ of the turbulence at $x=l_1$, the damping decrement $k_I(\omega)$ of the turbulence, grid locations l and l_1, and some plasma parameters are known. The power spectrum of the turbulence is assumed to be

$$S(\omega, \omega_0) = (\omega^2/4\omega_0^3)\exp(-|\omega|/\omega_0), \tag{12}$$

where ω_0 is related to f_c so that the auto-correlation time of the assumed turbulence equals the measured one. The simple form of Eq. (12) is a good approximation of the measured power spectrum, and furthermore, the value of F is not as sensitive to the form of the power spectrum as to the value of ω_0. The damping decrement of the turbulence has already been given by Eq. (11). Calculations were made for several values of the parameter β which characterizes the spatial damping of the turbulence.

The calculated values of η^2 are shown in Fig. 7 for four values of β around the measured one. The theoretical value of η^2 is chosen to be 3.4×10^{-5} so that the absolute value of $\eta^2 F$ fits the measured $K_i/\langle V_x^2\rangle$. Here, η^2 may range between 1.7×10^{-5} and 6.8×10^{-5} because of the error involved in phase velocity measurements. As described in Sec. II, the calculated values of $\eta^2 F$ are valid under the condition that v_s equal the phase velocity of the external turbulence, which was found to be 2.2×10^5 cm/sec as shown in Fig. 3. This condition is satisfied for $l_1 \simeq 14$ cm (i.e., $n_0^{1/3} l \simeq 1.3\times10^4$) where the saddle point velocity is calculated to be 2.1×10^5 cm/sec. And near this value of l_1, the theoretical curve with $\beta = 0.2$ agrees well with the experimental points in Fig. 7. The physical meaning of the measured l_1 dependence of the damping factor is that the streaming perturbation f_{ω_1} is more easily smoothed out by effective collisions because it becomes more highly oscillatory in v with increasing l_1.

Another example of calculations is given in Fig. 9. The curve with $\beta = 0$ does not fit the measured values especially when $f_c > 100$ kHz. The best agreement between the theory and the experiments is obtained when $\beta = 0.2$, which approximately coincides with the directly measured value of β. Namely, it is again confirmed that the turbulent ion waves do not exhibit linear Landau damping because of the relatively high amplitude of the applied noise signals. In Fig. 9, the same value of η^2 as in Fig. 7 is used in the calculations. In Fig. 2, we have shown the measured value of η^2 to be 6.18×10^{-5}. The quantitative agreement between measured and theoretical coupling coefficients η is extremely good in spite of the quite different methods used in their determinations.

Figure 9 shows that when f_c is not large, the damping factor per unit noise power becomes larger with f_c, and that this tendency reverses for $f_c > 100$ kHz. The reason is as follows. Since we kept the mean squared fluctuating potentials constant in varying the spectrum, the mean square of the turbulent electric fields becomes larger with broadening spectrum width on account of the wave number which is proportional to ω. Consequently, the velocity space diffusion of ions resulting from turbulent electric fields is enhanced for larger f_c. On the other hand, the turbulence decays more rapidly in space for higher frequencies than for the case of linear Landau damping. So, the total power of the turbulent electric fields decreases when the noise spectrum broadens beyond a critical value. The velocity space diffusion is thus reduced for f_c higher than the critical value, which was found to be about 100 kHz. From the viewpoint of plasma heating, it is concluded that the optimum band width of applied noise is 100 kHz for efficient ion heating in our experimental system.

It should also be noted that the damping factor per unit noise power is almost four times as large as that per unit power of monochromatic signals.

VI. CONCLUSIONS

The velocity space diffusion of ions due to effective collisions caused by externally applied noise signals was observed through the measurements of the amplitude of second order ion wave echoes.

It was revealed experimentally that the amplitude damping of echoes due to effective collisions depends sensitively on the power and the spectrum of the turbulence as well as on the location of the localized turbulence.

It was also found that the turbulent waves are far more effective than the monochromatic waves in increasing the effective collision frequency.

The numerical calculations of the damping factor of the echo amplitude were performed using the generalized quasi-linear Vlasov equation. From comparison with experimental results, it can be said that the generalized quasilinear theory used here is sufficient to explain the results, even quantitatively, in the case of weak turbulence.

ACKNOWLEDGMENTS

The authors wish to thank Professor H. Momota for valuable discussions on the theoretical problem, S. Kuwabara and T. Itoh for their preliminary work in this experiment, and Y. Sudoh for his assistance.

This research was supported in part by the Grant-in-Aid for Scientific Research from the Ministry of Education.

[1] S. M. Hamberger and J. Jancarik, Phys. Fluids **15**, 825 (1972); H. W. Hendel and J. T. Flick, Phys. Rev. Lett. **31**, 199 (1973).
[2] T. M. O'Neil and R. W. Gould, Phys. Fluids **11**, 134 (1968).
[3] T. M. O'Neil, Phys. Fluids **11**, 2420 (1968).
[4] J. H. Malmberg, C. B. Wharton, R. W. Gould, and T. M. O'Neil, Phys. Fluids **11**, 1147 (1968).
[5] C. Moeller, Phys. Fluids **18**, 89 (1975).
[6] H. Ikezi, T. Takahashi, and N. Nishikawa, Phys. Fluids **12**, 853 (1969).
[7] A. Y. Wong and D. R. Baker, Phys. Rev. **188**, 326 (1969).
[8] A. Sasaki and N. Sato, Phys. Fluids **15**, 1157 (1972).
[9] T. H. Jensen, J. H. Malmberg, and T. M. O'Neil, Phys. Fluids **12**, 1728 (1969).
[10] M. Guillemot, J. Olivain, F. Perceval, A. Quemeneur, and G. Matthieussent, in *Proceedings of the Third International Conference on Quiescent Plasmas* (Danish Atomic Energy Commission Riso, Denmark, 1971), p. 275.
[11] N. Sato and A. Sasaki, J. Phys. Soc. Jpn. **32**, 543 (1972).
[12] Y. Yasaka, Y. Sudoh, and R. Itatani, J. Phys. Soc. Jpn. **38**, 1793 (1975).